

1 Estimating aquifer hydraulic properties from the inversion of surface 2 Streaming Potential (SP) anomalies

3 Mathieu Darnet, Guy Marquis, and Pascal Sailhac

4 Ecole et Observatoire des Sciences de la Terre, Institut de Physique du Globe, Strasbourg, France

5 Received 28 April 2003; accepted 28 May 2003; published XX Month 2003.

6 [1] Electrokinetic effects of water flow during pumping
7 tests have been shown to generate surface Streaming
8 Potential (SP) anomalies of several tens of mV that are well
9 correlated with the geometry of the water table. It follows that
10 SP measurements can be used to estimate aquifer hydraulic
11 properties. We have developed an inversion scheme for
12 surface SP data generated by flow pumping and found that we
13 are able to estimate the hydraulic conductivity and the depth
14 and the thickness of the aquifer. We applied our inversion
15 scheme to the data from *Bogoslovsky and Ogilvy* [1973] and
16 found a hydraulic conductivity of 10^{-5} m.s^{-1} , an aquifer
17 thickness of roughly 28 m and an electrokinetic coupling
18 coefficient of -1 mV.m^{-1} . These values are in the range of
19 what is expected for this kind of environment. INDEX

20 TERMS: 1829 Hydrology: Groundwater hydrology; 0925
21 Exploration Geophysics: Magnetic and electrical methods; 5109
22 Physical Properties of Rocks: Magnetic and electrical properties.
23 Citation: Darnet, M., G. Marquis, and P. Sailhac, Estimating
24 aquifer hydraulic properties from the inversion of surface
25 Streaming Potential (SP) anomalies, *Geophys. Res. Lett.*, 30(0),
26 XXXX, doi:10.1029/2003GL017631, 2003.

29 1. Introduction

30 [2] Field estimates of aquifer hydraulic properties require
31 the use of several expensive observation wells. An alterna-
32 tive is to use minimally invasive geophysical methods to
33 estimate groundwater fluxes. Standard methods (e.g., elec-
34 trical sounding, ground-penetrating radar, time-domain elec-
35 tromagnetic methods) detect the presence of water by
36 changes of ground physical properties (e.g., electrical con-
37 ductivity, dielectric permittivity) but none of them are
38 sensitive to actual water flow, except the Streaming Poten-
39 tial (SP) method. Indeed, the SP method measures with
40 electrodes the natural electric potential variations that in-
41 clude those generated by the electrokinetic effect of under-
42 ground fluid flow. Thus, the distribution of the electric
43 potentials allows us to map groundwater flow features
44 [e.g., *Corwin and Hoover*, 1979].

45 [3] In the case of water pumping, the electrokinetic effect
46 generates surface SP anomalies of several tens of mV that
47 are very well correlated to the geometry of the water table
48 [*Bogoslovsky and Ogilvy*, 1973, *Kelly and Mares*, 1993].
49 Therefore, can we use the SP technique for estimating
50 hydraulic properties of the aquifer?

51 [4] To investigate this matter, several potential-field
52 inversion techniques are available. All these techniques
53 describe either the shape of the water table [*Fournier*,

1989; *Birch*, 1998] or the location and/or the shape of the
54 electrokinetic sources [*Patella*, 1997; *Sailhac and Marquis*,
55 2001; *Revil et al.*, 2003] but none of these describes
56 completely the geometry of the aquifer, especially its thick-
57 ness. We have therefore developed a new inversion scheme
58 of surface SP data obtained during flow pumping to estimate
59 the aquifer hydraulic properties (thickness, depth and
60 hydraulic conductivity). We tested our approach on the SP
61 and hydraulic data sets from *Bogoslovsky and Ogilvy* [1973]
62 to estimate the resolution of each hydraulic parameter. 63

2. Inversion Scheme of Surface SP Anomalies Induced by Water Pumping

2.1. Hydraulic Model

64 [5] Our inversion scheme for surface SP anomalies is
65 based on a forward model of the electrokinetic effect of
66 pumping in a homogeneous unconfined aquifer. This SP
67 modeling is a three-step process that consists in solving the
68 hydraulic problem, computing the streaming current sources
69 and solving the electric problem. 70
71

72 [6] We assumed that the water flow occurs in a homoge-
73 neous unconfined aquifer in steady-state conditions limited
74 at the bottom by impermeable bedrock. We assumed that the
75 bedrock is horizontal and hence so is the flow (Dupuit's
76 hypothesis). Moreover, we assumed that the flow is radial,
77 that the water flux around the well is equal to the pumping
78 flow rate Q and that the piezometric head in the vicinity of
79 the well (at r_0) is h_0 (Figure 1). Under these assumptions, the
80 solution of (1) is for $r > r_0$ [*De Marsily*, 1986] 81

$$h(r) = \sqrt{h_0^2 + \frac{Q}{\pi K} \ln(r/r_0)} \quad (1)$$

82 where h is the piezometric head (m) and K is the aquifer
83 hydraulic conductivity (m.s^{-1}). 84

2.2. Electric Current Sources Calculation

85 [7] The second step is to convert the modeled piezomet-
86 ric head h into electrokinetic current sources I_s . For this
87 purpose, we used the electric current conservation equation
88 [cf. e.g., *Revil et al.*, 1999] 89

$$\nabla \cdot (\sigma \nabla V) = -(\nabla L \cdot \nabla P + L \nabla^2 P) \quad (2)$$

90 where P is the fluid pressure (Pa), V is the electric potential
91 (V), L is the electrokinetic coupling parameter
92 ($\text{V.S.Pa}^{-1}.\text{m}^{-1}$) and σ the ground electrical conductivity
93 (S.m^{-1}). L depends mainly on the rock lithology and the
94 fluid chemistry [*Revil et al.*, 1999]. Let us assume that the
95 soil and the fluid are homogeneous and hence that L is
96 constant, so the first term of the right hand side of equation
97 (4) is negligible. 98

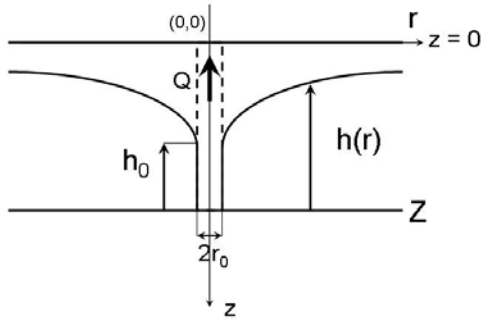


Figure 1. Sketch of the unconfined aquifer used to model the electrokinetic effect of a pumping test.

[8] Instead of using fluid pressure, we prefer to use the piezometric head ($h = P/\rho g$) and (4) can be written as

$$\vec{\nabla} \cdot (\sigma \vec{\nabla} V) = -L \nabla^2 P = -\rho g L \nabla^2 h \quad (3)$$

where ρ is the fluid density (kg.m^{-3}) and g is the gravity acceleration (m.s^{-2}). In this equation, the source term on the right hand side can be interpreted as electrokinetic current sources I_s (A.m^{-3}). Combining (3) and (5), we get

$$I_s = -\rho g \nabla^2 h = \frac{\rho g L Q^2}{4\pi^2 K^2 r^2 \left(h_0^2 + \frac{Q \ln(r/r_0)}{\pi K} \right)^{3/2}} \quad (4)$$

2.3. Electrical Model

[9] The final step is to compute the electric potential distribution V by solving the electric current conservation equation (5) knowing the ground electrical conductivity distribution. In well pumping experiments, the high electrical conductivity of the metal casing disturbs the electric field near the wells. *Ishido et al.* [1983] proposed that the metal casing was channeling the electric currents generated at reservoir depth to the surface and hence to the surface electrodes. Therefore, our electrical conductivity model is a homogeneous half-space with a high-conductivity vertical cylindrical body representing the casing. We did not take into account the drop of electrical conductivity at the top of water table caused by water content decrease in the vadose zone because it is a second-order effect less than two orders of magnitude [e.g., *Revil et al.*, 1999] compared to the electrical conductivity contrast between the casing and the host-medium more than eight orders of magnitude [e.g., *Schenkel and Morrison*, 1990].

[10] We solve this problem using an integral formulation [Schenkel and Morrison, 1990] that gives a numerical estimate of the casing Green function G as a function of the ground and casing electrical conductivities and of the casing length, radius and thickness. G is obtained numerically by solving the electric current conservation equation (5) in both the half-space and the casing. Therefore, by integrating all electrokinetic sources induced by the water pumping (equation 6), we get the solution of (5) at the ground level,

$$V(r, z = 0) = \int_0^\infty \int_0^{2\pi} \int_{Z-h(r')}^Z G(r, z = 0, r', \theta', z') I_s(r', z') r' dz' d\theta' dr' \quad (5)$$

The vertical integration is limited to the aquifer thickness because $I_s = 0$ outside the aquifer.

2.4. Inversion of SP Data

[11] Equation (7) describes the surface SP anomaly induced by a pumping test at rate Q in an unconfined homogeneous aquifer of hydraulic conductivity K , electrokinetic coupling parameter L and bedrock depth Z . Therefore, knowing the hydraulic head h_0 in the vicinity of the well (at r_0) and the surface SP anomaly during a pumping test of flow rate Q , we should be able to determine Z , K , and L . We used a genetic algorithm [Dorsey and Mayer, 1995] to find the best $\{Z, K, L\}$ that minimizes a weighted quadratic error function f between the predicted and observed SP data

$$f = \sqrt{\frac{1}{N} \sum_{i=1}^N w_i (V_{0i} - V_{Pi})^2} \quad (6)$$

where N is the number of measurements, w_i is the weight of measurement i ($0 < w_i < 1$) and V_{0i} and V_{Pi} are respectively the observed and predicted SP data i .

3. Application to the Inversion of Bogoslovsky and Ogilvy [1973] Data Set

[12] During a long-term pumping experiment, *Bogoslovsky and Ogilvy* [1973] have recorded simultaneously the surface SP anomaly and piezometric heads at nine observation wells (Figure 2). They observed a very good correlation between these two profiles that they attributed to the electrokinetic effect of the groundwater flow. Besides, two negative anomalies (at -65 and 110 m) were recorded above drainage ditches certainly caused by water infiltration.

[13] We performed an inversion of the SP data from only one side of well because our model requires a cylindrical

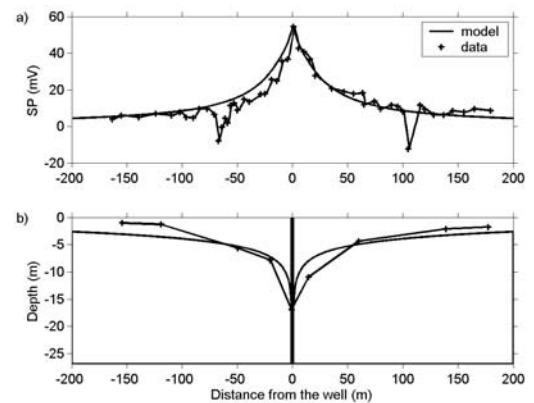


Figure 2. Result of the inversion of SP data from *Bogoslovsky and Ogilvy* [1973]. (a) Modeled (solid line) and recorded (cross line) surface SP anomaly. (b) Modeled (solid line) and recorded (cross line) piezometric heads. We found a bedrock depth of $Z = 28$ m, a ratio of the flow rate and the hydraulic conductivity $Q/K = 290 \text{ m}^2$ and an electrokinetic coupling parameter $L = 0.8 \text{ mV.S.MPa}^{-1} \cdot \text{m}^{-1}$ ($C = -0.8 \text{ mV.m}^{-1}$).

168 symmetry; we used here the data that have positive abscissa.
 169 We assumed that the piezometric head at the well (h_0) was
 170 equal to the piezometric head recorded by the authors close
 171 to the well [i.e., -17 m (Figure 2)]. We chose weights of 1
 172 for measurements located closer than 50 m from the well
 173 and of 0.5 further than 50 m to increase the influence of the
 174 significant measurements close to the well. We chose a
 175 weight of 0 for the small negative anomaly because it is not
 176 related to the pumping. For this inversion, we assumed that
 177 the casing length is 20 m, the inner radius 9 cm, the
 178 thickness 1.3 cm, the electrical conductivity 10^8 S.m $^{-1}$
 179 and the host medium electrical conductivity 100 Ω .m that
 180 are typical values for pumping casings [Schenkel and
 181 Morrison, 1990] in shallow formations like sandy gravels
 182 [Aleshin et al., 1969].

183 [14] We found a bedrock depth of $Z = 28$ m, a ratio of the
 184 flow rate and the hydraulic conductivity $Q/K = 290$ m 2 and an
 185 electrokinetic coupling parameter $L = 0.8$ mV.S.MPa $^{-1}$.m $^{-1}$.
 186 We show the result of inversion on Figure 2 where for sake of
 187 comparison, we plotted the observed and predicted SP data
 188 (Figure 2a) and the observed and predicted hydraulic heads
 189 (Figure 2b).

190 [15] We obtained a satisfactory fit of the trend of hydraulic
 191 heads (Figure 2a). Nevertheless, this fit is not perfect
 192 because our inversion does not take into account local
 193 hydraulic or electrical conductivity heterogeneities. As we
 194 do not know the pumping flow rate, we can only estimate
 195 K: assuming a typical flow rate value of few cubic meters
 196 per hour (e.g., 10 m 3 .h $^{-1}$) we found a hydraulic conductivity
 197 of around 10^{-5} m.s $^{-1}$; this is in agreement with what is
 198 expected for sandy gravels for which K ranges from 10^{-5} to
 199 10^{-3} m.s $^{-1}$ [De Marsily, 1986]. We found an electrokinetic
 200 coupling parameter L of 0.8 mV.S.MPa $^{-1}$.m $^{-1}$ but to ease
 201 comparison with published values, we prefer to use the
 202 electrokinetic coupling coefficient C in mV.m $^{-1}$

$$C = -\frac{\rho g L}{\sigma} \quad (7)$$

204 where σ is the ground electrical conductivity. We found a C
 205 of -0.8 mV.m $^{-1}$, a reasonable value since C is usually in
 206 the range of -1 to -10 mV.m $^{-1}$ for typical groundwater
 207 [Revil et al., 2002].

208 4. Discussion

209 4.1. Robustness of the Inversion

210 [16] To investigate the robustness of the inversion, we
 211 have performed 125 successive inversions of the SP data.
 212 Each inversion stopped when the optimal solution did not
 213 change for 40 generations. The histograms of the different
 214 solutions are shown in Figure 3. The values of Z are
 215 clustered within 2% of its mean value, Q/K within 7% for
 216 and C within 13%. These small values indicate that the
 217 genetic algorithm gives similar solutions even though it
 218 explores a wide parameter space (shown by the abscissae of
 219 Figure 3).

220 4.2. Sensitivity of the Inversion

221 [17] To investigate the reliability of our inversion of SP
 222 data, we tested the sensitivity of the quadratic error function
 223 f to each parameter (Z, Q/K or C). As during pumping the
 224 flow rate Q is obviously known, we prefer to use K instead

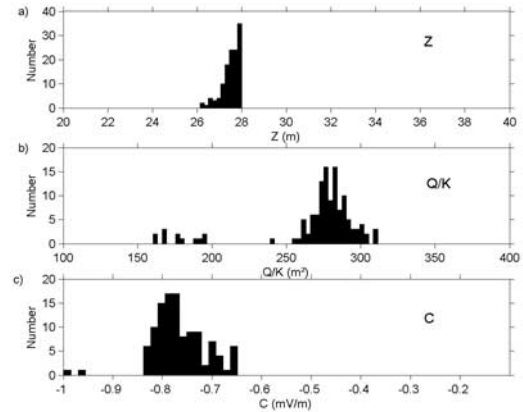


Figure 3. Distribution of the solutions found from 125 inversions of the SP data: (a) depth of the aquifer bedrock, (b) ratio flow rate Q above the hydraulic conductivity K and (c) electrokinetic coupling coefficient.

of Q/K; for this purpose, we chose as previously an arbitrary 225
 value of 10 m 3 .h $^{-1}$ for Q. 226

227 [18] We fixed two out of three parameters to their values
 228 obtained in the best-fitting model and set free the third
 229 parameter. The result is shown on Figure 3 where we plotted
 230 the quadratic error function f as function of Z (Figure 3a),
 231 the logarithm of K (Figure 3b) and C (Figure 3c). We chose
 232 to use the logarithm of K instead of K because it can easily
 233 vary over several orders of magnitude for shallow
 234 formations. The gradient of the error function f around the
 235 minimum gives an idea of resolution of each parameter: the
 236 strongest the gradient, the better the parameter. We found a
 237 resolution of 2 mV/m for Z, on average 50 mV/log(m/s) for
 238 K and 8 mV/(mV/m) for C. The best determined parameter
 239 is therefore the hydraulic conductivity K (or the ratio Q/K),
 240 followed by the coupling coefficient C and the bedrock
 241 depth Z. K is well determined because the electrokinetic
 242 current source term I_s depends on K squared (equation 6). C
 243 is also relatively well defined because it acts as a
 244 multiplicative factor of I_s . On the contrary, Z is poorly
 245 resolved because it only appears in the integration domain
 246 of equation (7) and does not affect the intensity of I_s
 247 (equation 6). Moreover, for great Z values, the additional
 248 sources have negligible effects at the surface, hence the low
 249 variation rate of f for large Z values (Figure 3a).

250 [19] Figure 3b shows that if we can estimate C (e.g., from
 251 laboratory tests on samples) and Z (e.g., from drilling or
 252 seismic method), we can reasonably expect to estimate the
 253 hydraulic conductivity from the inversion of surface SP data.
 254 However, as C depends on the chemistry of the water/rock
 255 interaction [Revil et al., 1999], it can change dramatically
 256 within the same aquifer depending on the lithology and the
 257 water composition. Moreover, the depth of bedrock Z is also
 258 a parameter difficult to obtain because in real cases the
 259 bedrock is not horizontal and even sometimes discontinu-
 260 ous. Therefore, we can not expect to know very well C and
 261 Z for real cases and consequently, the accuracy on K will
 262 not be as good as than what is shown on Figure 3b.

263 [20] To improve the accuracy on Z, C and hence on K, we
 264 propose to over-determine the inversion problem by
 265 performing a joint inversion of several SP data sets acquired
 266 during pumping tests at different rates. Indeed, each test

267 should provide new information on the system as the SP
 268 response is a function of Q (equation 6). *Kawakami and*
 269 *Takasugi*, [1994] actually observed such a behavior during
 270 injection and production tests in a geothermal reservoir:
 271 they observed that the surface SP anomalies change their
 272 sign according to the flow direction and that they increase
 273 with the flow rate. Therefore, several hydraulic tests at
 274 different flow rates should give redundant information on Z ,
 275 C , and K that should improve greatly the accuracy on Z , C ,
 276 and K .

277 4.3. Surface SP: A Mirror Image of the Water Table?

278 [21] In our inversion, we assumed that the flow was radial
 279 around the well but it is obviously not the case as we can
 280 observe it on the hydraulic heads profiles on each side of the
 281 well (Figure 2b). This asymmetry seems related to the
 282 asymmetry of the surface SP data (Figure 2b) and explains
 283 why *Bogoslovsky and Ogilvy* [1973] concluded that “the
 284 natural electric field may be regarded as a mirror image of
 285 the cone surface”. The more likely explanation for this SP
 286 asymmetry is that before pumping, the aquifer is not at
 287 equilibrium because away from the well, the piezometric
 288 head is higher on the left side than on the right side.

289 [22] This good correlation between both electric and
 290 hydraulic potentials can be explained by the fact that the
 291 fundamental equations governing both potentials are both
 292 diffusion equations (1) and (4) with sources roughly located at
 293 the same place (i.e., at the openhole). Indeed, as the electro-
 294 kinetic sources vary roughly in radius squared (cf. equation 6),
 295 we can assume that they are concentrated around the well.

296 [23] The electrical conductivity model of our inversion
 297 takes into account a highly electrically conductive steel
 298 casing that is channeling the electric currents to the surface.
 299 Figure 4 shows the distribution of the normalized electric
 300 currents generated by the electrokinetic effect of the pump-
 301 ing. We can clearly observe that the surface SP anomaly is
 302 caused by the electric currents coming from the casing.
 303 There are therefore no direct relationship between the
 304 surface SP anomaly and the shape of the water table as
 305 suggested by *Bogoslovsky and Ogilvy* [1973]. We point out
 306 that all SP analysis methods based on Fournier’s integral
 307 formula [*Fournier*, 1989; *Birch*, 1998; *Revil et al.*, 2002]

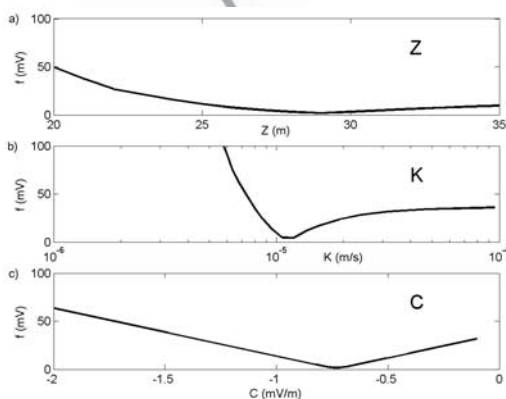


Figure 4. Quadratic error function f between observed and predicted SP data as a function of (a) Z , (b) $\log K$ and (c) C . The gradient of the error function f around the minimum gives an idea of resolution of each parameter: the strongest the gradient, the better the estimate.

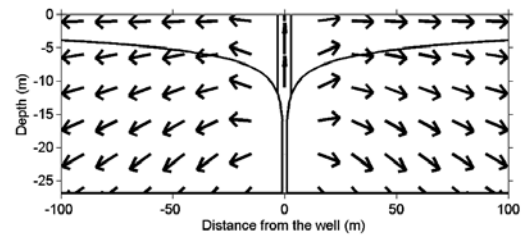


Figure 5. Distribution of electric currents normalized to their intensities generated by water flow during pumping. Note that the surface SP anomaly is caused by the electric currents coming from the reservoir through the steel casing situated at distance = 0.

308 assume that the ground electrical conductivity above the
 309 aquifer is constant; they can therefore not be applied for
 310 quantifying the shape of the water table when highly
 311 electrically conductive casings are buried in the ground.

312 [24] Tomographic algorithms of *Patella* [1997] and *Revil*
 313 *et al.* [2003] give a source depth of around 5 m that is much
 314 shallower than the true depth of the SP sources (between 17
 315 and 25 m). This discrepancy is caused by the fact that these
 316 techniques are as sensitive to the ground electrical
 317 conductivity contrasts as to the SP source location; they
 318 can therefore not be applied for locating the SP source when
 319 the well is steel-cased.
 320

321 5. Conclusions and Perspectives

322 [25] Our inversion scheme of Streaming Potential (SP)
 323 anomalies induced by water pumping allows us to give an
 324 estimate of the hydraulic conductivity and of the geometry
 325 of an aquifer. As it takes into account the presence of highly
 326 electrically conductive steel casings that channel the electric
 327 currents to the surface, it generalizes standard SP analysis
 328 methods.

329 [26] To improve the accuracy of the parameter estimates,
 330 we propose to perform a joint inversion of SP monitoring
 331 data acquired during pumping tests at different rates. How-
 332 ever, this approach would require rewriting the proposed
 333 steady-state equations in their transient expressions. Never-
 334 theless, this would allow to gain more insight into the
 335 transient regime of the pumping and therefore to get an
 336 estimate of the specific storage coefficient of the aquifer.
 337 Furthermore, time monitoring of SP data effectively
 338 removes any static effect caused by electrical conductivity
 339 contrasts, e.g., due to a casing as suggested by *Marquis et*
 340 *al.* [2002], and therefore to allow us the localization of the
 341 electrokinetic sources. Thus, surface SP monitoring can
 342 provide a picture of the groundwater flow distribution and
 343 perhaps allows to identify ground hydraulic conductivity
 344 heterogeneities without in-situ measurements.

345 [27] **Acknowledgments.** This study benefited from a grant INSU-
 346 CNRS ‘Programme National de Recherche en Hydrologie (PNRH)’. MD
 347 wishes to acknowledge financial support from joint CNRS-Région Alsace
 348 doctoral fellowship. We want to thank Philippe Ackerer from the Institut de
 349 Mécanique des Fluides de Strasbourg for his fruitful discussions. We also
 350 want to thank the two referees and the editor for their fruitful comments.

351 References

352 Aleshin, A. S., Yu. I. Baulin, V. A. Bogoslovsky, and A. A. Ogilvy, Geo-
 353 physical observations of vertical drainage operation in the Arazdayan
 354 steppe, *Gidrotechnika i melioratsiya*, No. 5, 82–90, 1969.
 355

- 355 Birch, F. S., Imaging the water table by filtering self-potential, *Ground*
 356 *Water*, 36, 779–782, 1998.
- 357 Bogoslovsky, V. A., and A. A. Ogilvy, Deformations of natural electric
 358 fields near drainage structures, *Geophys. Prospect.*, 21, 716–723, 1973.
- 359 Corwin, R. F., and D. B. Hoover, The Self-Potential method in geothermal
 360 exploration, *Geophysics*, 44, 226–245, 1979.
- 361 De Marsily, G., *Quantitative hydrogeology*, 85–89, Academic Press Inc.,
 362 London, 1986.
- 363 Dorsey, R. E., and W. J. Mayer, Genetic algorithms for estimation problems
 364 with multiple optima, nondifferentiability, and other irregular features,
 365 *J. Bus. Econ. Stat.*, 13(1), 53–66, 1995.
- 366 Fournier, C., Spontaneous potentials and resistivity surveys applied to
 367 hydrogeology in a volcanic area: case history of the Chaîne des
 368 Puys (Puy-de-Dôme, France), *Geophys. Prospect.*, 37, 647–668,
 369 1989.
- 370 Ishido, T., H. Mizutani, and K. Baba, Streaming Potentials observations
 371 using geothermal wells and in situ electrokinetic coupling coefficients
 372 under high temperature, *Tectonophysics*, 91, 89–104, 1983.
- 373 Kawakami, N., and S. Takasugi, SP monitoring during the hydraulic frac-
 374 turing of the TG-2 well, *Extended Abstracts of Papers, EAGE-56th Meet-*
 375 *ing, 1004*, 1994.
- 376 Kelly, W. E., and S. Mares, Applied geophysics in hydrogeological and
 377 engineering practice, *Elsevier Science*, 86–87, 1993.
- 378 Marquis, G., M. Darnet, P. Sailhac, A. K. Singh, and A. Gerard, Sur-
 379 face electric variations induced by deep hydraulic stimulation: An
 example from the Soultz HDR site, *Geophys. Res. Lett.*, 29(14), 380
 71–74, 2002. 381
- Patella, D., Introduction to ground surface self-potential tomography, *Geo-*
 382 *phys. Prospect.*, 45, 653–681, 1997. 383
- Revil, A., H. Schwaeger, L. M. Cathles III, and P. D. Manhardt, Streaming
 384 potential in porous media, 2. Theory and application to geothermal sys-
 385 tems, *J. Geophys. Res.*, 104, 20,033–20,048, 1999. 386
- Revil, A., D. Hermitte, M. Voltz, R. Moussa, J.-G. Lacas, G. Bourrié, and
 387 F. Trolard, Self-Potential signals associated with variations of the hydrau-
 388 lic head during an infiltration experiment, *Geophys. Res. Lett.*, 29(7),
 101–104, 2002. 389
- Revil, A., V. Naudet, J. Nouzaret, and M. Pessel, Principles of electrogra-
 391 phy applied to self-potential electrokinetic sources and hydrogeological
 392 applications, *Water Resour. Res.*, doi 2002WR000916, 2003. 393
- Sailhac, P., and G. Marquis, Analytic potentials for the forward and inverse
 394 modeling of SP anomalies caused by subsurface fluid flow, *Geophys.*
 395 *Res. Lett.*, 28, 1643–1646, 2001. 396
- Schenkel, C. J., and H. F. Morrison, Effects of well casing on potential field
 397 measurements using downhole current sources, *Geophys. Prospect.*, 38,
 663–686, 1990. 399
- M. Darnet, G. Marquis, and P. Sailhac, Ecole et Observatoire des 401
 Sciences de la Terre, Institut de Physique du Globe, UMR 7516, 5 rue René 402
 Descartes, 67084, Strasbourg, France. (Mathieu.Darnet@eost.u-strasbg.fr) 403